Food and Chemical Toxicology 132 (2019) 110661

Contents lists available at ScienceDirect

Food and Chemical Toxicology

journal homepage: www.elsevier.com/locate/foodchemtox

DNA methylation is involved in pro-inflammatory cytokines expression in T-2 toxin-induced liver injury

Aimei Liu[a], Yaqi Sun[a], Xiaojing Wang[a], Awais Ihsan[d], Yanfei Tao[c], Dongmei Chen[b], Dapeng Peng[c], Qinghua Wu[e,**], Xu Wang[a,b,*], Zonghui Yuan[a,b,c]

[a] National Reference Laboratory of Veterinary Drug Residues (HZAU) and MAO Key Laboratory for Detection of Veterinary Drug Residues, Huazhong Agricultural University, Wuhan, Hubei, 430070, China
[b] MOA Laboratory for Risk Assessment of Quality and Safety of Livestock and Poultry Products, Hubei, 430070, China
[c] Hubei Collaborative Innovation Center for Animal Nutrition and Feed Safety, Wuhan, China
[d] Department of Biosciences, COMSATS University Islamabad, Sahiwal Campus, Pakistan
[e] Department of Chemistry, Faculty of Science, University of Hradec Kralove, Hradec Kralove, 50003, Czech Republic

ARTICLE INFO

Keywords:
T-2 toxin
DNA methylation
Pro-inflammatory cytokine
Hepatotoxicity

ABSTRACT

Currently, T-2 toxin has been reported to cause liver toxicity with the effects of oxidative stress and inflammation; however, the underlying mechanism of T-2 toxin-induced liver injury is not fully understood. Increasing lines of evidence show that DNA methylation affects the expression of inflammatory cytokine, and plays a crucial role in autoimmune diseases. Nevertheless, the potential role of DNA methylation in the hepatotoxicity of T-2 toxin has not been explored. In this study, female Wistar rats were given a single dose of T-2 toxin at 2 mg/kg b.w. and were sacrificed at 1, 3 and 7 days post-exposure. *In vitro*, a normal rat liver cell line (BRL) was exposed to different concentrations of T-2 toxin. Histopathological analysis was used to investigate damage to the liver, which was detected at the molecular level by RT-PCR, Western blot and immunohistochemical assays, methylation-specific PCR (MSP), bisulfite sequencing (BSP), and flow cytometry. The results showed that T-2 toxin significantly increased the levels of DNA methyltransferases (DNMT1, DNMT3A), which were mainly concentrated at the site of liver injury. The 5-methylcytosine (5-mC) level of genomic DNA was also raised in T-2 toxin-treated rat livers. The expression of inflammatory cytokines (IL-6, IL-1β, IL-11, IL-1α, and TNF-α) increased both *in vivo* and *in vitro* under T-2 toxin treatment. Notably, DNA demethylation directly increased the expression of cytokines IL-11, IL-6, IL-α, and TNF-α under T-2 toxin exposure. DNA methylation inhibitors combined with T-2 toxin directly or indirectly induced the production of inflammatory cytokines and aggravate cell apoptosis. Our study uncovered for the first time that DNA methylation is related to the expression of inflammatory cytokines in T-2 toxin-induced liver injury. These findings suggested that DNA methylation is a potential mechanism of T-2 toxin-induced hepatotoxicity.

1. Introduction

As one of the most toxic trichothecenes mycotoxins produced by species of *Fusarium*, T-2 toxin is highly concerned in most countries (Deng et al., 2018). T-2 toxin contaminates human food, animal feeds, and agricultural products such as wheat, maize, and barley (Hjelkrem et al., 2018; Matejova et al., 2017). The contamination of T-2 toxin is a serious problem in many countries, including China (Wang et al., 2018b), America (Garrido et al., 2013), Britain (Lawson et al., 2018), Spain, Italy and France (Paterson et al., 2018). For instance, a study in Italy found that 100% of barley samples had contamination, with an average T-2 toxin level of 443 μg/kg and the highest level reaching 724 μg/kg (Morcia et al., 2016). For instance, a study in Italy found that 100% of barley samples were contaminated with an average T-2 toxin level of 443 μg/kg and the highest level of 724 μg/kg (Zhang et al., 2018a). The exposure of T-2 toxin damages hippocampal neurons (Tanaka et al., 2016), causes animal vomiting (Wu et al., 2016). Importantly, the chronic exposure of T-2 toxin was associated with liver injury (Slobodchikova and Vuckovic, 2018).

The current literature has also shown the relationship of liver toxicity with T-2 toxin. T-2 toxin-treated rats exhibited a significant decrease in relative liver weights (Tamimi et al., 1997). Shinozuka et al.

* Corresponding author. Huazhong Agricultural University, Wuhan, Hubei, 430070, China.
** Corresponding author. College of Life Science, Yangtze University, Jingzhou, 434025, China.
E-mail addresses: wqh212@hotmail.com (Q. Wu), wangxu@mail.hzau.edu.cn (X. Wang).

https://doi.org/10.1016/j.fct.2019.110661
Received 23 March 2019; Received in revised form 22 June 2019; Accepted 2 July 2019
Available online 03 July 2019

reported that the levels of plasma aspartate aminotransferase (AST) and alanine aminotransferase (ALT) were increased after a single oral dose of 10 mg/kg b.w. to mice for 2 days, and T-2 toxin caused considerable damage to hepatocytes through apoptosis (Shinozuka et al., 2009). In another study, an incubation of T-2 toxin (at 46.6, 233 and 466 ng/ml) for 24 and 42 h could decrease liver microsomal protein, liver DNA levels, glycogen levels and increase liver RNA levels in porcine mononuclear cells (Horvatovich et al., 2013). Importantly, the production of pro-inflammatory cytokines were also observed in the T-2 toxin-induced hepatotoxicity (Luo et al., 2018). However, the role of pro-inflammatory factors in T-2 toxin-induced liver injury, which could provide a basis for the prevention and treatment of T-2 toxin-induced hepatotoxicity, remains unclear.

Pro-inflammatory cytokines might play important roles in T-2 toxin-induced injury (Li et al., 2013; Ravindran et al., 2011; Zhou et al., 2014). Previous research showed that T-2 toxin could promote pro-inflammatory cytokines, including IL-1β and TNF-α in chondrocytes, and thus aggravate kashin-beck disease (KBD) (Li et al., 2008; Zhou et al., 2014). T-2 toxin elevated the levels of pro-inflammatory cytokines, IL-1β, IL-1α, IL-6 and TNF-α in the brain and spleen, and caused an alteration in blood-brain barrier (BBB) (Ravindran et al., 2011). Recent studies further revealed that pro-inflammatory cytokines IL-1β, IL-6, IL-11, and TNF-α play a critical role in the cytotoxicity of T-2 toxin in GH3 and RAW264.7 cells, causing cell apoptosis and growth inhibition (Liu et al., 2017a).

Other studies have shown that DNA methylation can modulate the expression of inflammatory cytokines. Conventionally, DNA methyltransferases (DNMT1, DNMT3A, and DNMT3B) can control the level of DNA methylation, particularly including 5-mC, and these enzymes are closely related to the expression of inflammatory cytokines. Increased levels of DNMT1 could enhance the release of lipopolysaccharide (LPS)-induced pro-inflammatory cytokines, such as TNF-α and IL-6 in macrophages (Cheng et al., 2014). DNMT3A overexpression could increase DNA methylation in the IL-6 promoter in synovial fibroblasts (Yang et al., 2017). Additionally, the abnormal methylation levels of pro-inflammatory factors, such as IL-6, TNF-α, IL-1α, and IL-11 promoters, can alter the expression level of these genes and promote the inflammatory response (Arroyo-Jousse et al., 2016; Notley et al., 2017). However, the role of DNMT1 and DNMT3A in T-2 toxin-induced hepatotoxicity has not been identified, and the relationship between DNA methylation and inflammatory factors under T-2 toxin remains to be determined.

From previous studies, we hypothesize that DNA methylation is a potential mechanism of T-2 toxin-induced inflammatory cytokine production in liver cell injury. This study was conducted to investigate the role of DNA methyltransferases and pro-inflammatory cytokines in rat liver injury after treatment with T-2 toxin, as well as how genome methylation patterns and methylation level of pro-inflammatory cytokine promoter regions were altered after rat livers or BRL cells are exposed to T-2 toxin *in vivo* and *in vitro*.

2. Materials and methods

2.1. Reagents and chemicals

T-2 toxin (CAS NO. 21259-20-1), 3-(4, 5-dimethyl thiazolyl-2)-2, 5-diphenyltetrazolium bromide (MTT), bovine serum albumin (BSA), RIPA lysis buffer, thiourea, phenylmethanesulfonyl fluoride (PMSF), sodium dodecyl sulphate (SDS), 5-Aza-2′-deoxycytidine (DAC), Universal Genomic DNA Kit, glutamine, acrylamide, bis-acrylamide, ammonium persulfate (APS), Tris Base, DL-Dithiothreitol (DTT), methanol and dimethylsulfoxide (DMSO) were purchased from Sigma (St. Louis, MO, USA). High-glucose DMEM was obtained from Hyclone (Logan, UT, USA); fetal bovine serum (FBS), antibiotics (penicillin, streptomycin) and trypsin-EDTA solution were supplied by Gibco BRL-Life Technologies (Logan, UT, USA). M-MLV RTase, dNTP Mixture (10 mM), 5 × M-MLV buffer, Oligo d(T)18, RNAiso Plus, SYBR Premix Ex Taq™ (Perfect Real Time) were bought from TaKaRa Biotechnology Co., Ltd. (Dalian, Liaoning, P.R. China). DAPI Staining Solution was bought from Beyotime (Wuhan, P.R. China). MethylFlash Methylated DNA Quantification Kit (Colorimetric) was purchased from Epigentek (Farmingdale, NY, USA). The EZ DNA Methylation-Gold™ Kit and Zymo Taq™ PreMix were purchased from Zymo Research Corp (Orange, CA, USA). DNMT1 (D63A6) XP® Rabbit mAb was purchased from Cell Signalling Technology (Mass, USA). IL-6, IL-1β, IL-11, and DNMT3A antibodies were purchased from Abcam (Cambridge England). The Annexin V/Propidium Iodide (PI) Apoptosis Kit was obtained from BestBio (Shanghai, P.R. China).

2.2. Animals and cells culture

Specific pathogen free female Wistar rats, weighing between 150 and 200 g, from the Centre of Laboratory Animals of Hubei Province, Wuhan, P.R. China, were used for this study. The study was approved by the Ethical Committee of the Faculty of Veterinary Medicine (Huazhong Agricultural University, Wuhan, P.R. China). Animals were kept in well-maintained animal rooms at a temperature of 20–26 °C, with a relative humidity of 40–70% and a 12 h light/dark cycle. During the first week of the acclimatization period, all animals received basic feed and fresh water. Four rats were housed per cage with hardwood shavings as bedding.

The normal rat liver cell line (BRL) was purchased from the Cell Bank of Type Culture Collection at the Chinese Academy of Sciences. BRL cells were cultured in DMEM supplemented with 10% FBS, 2 mmol/L glutamine, 100 U/mL penicillin, and 100 μg/mL streptomycin at 37 °C with an atmosphere of 5% CO_2. BRL cells passaged 5–15 times were used in the experiments. All experiments were performed at least in triplicate on three separate occasions.

2.3. Experimental design

T-2 toxin was dissolved in DMSO and then was diluted in phosphate buffered saline (PBS). For the time course study, animals were divided into four groups containing five animals at each time point (0 h, 1, 3 and 7 days). The oral LD_{50} of T-2 toxin in female rats is 7.0 mg/kg b.w. (Fairhurst et al., 1987). Several studies have illuminated that acute injury of the spleen, liver, brain and pituitary was observed in rats exposed to 2 mg/kg b.w. T-2 toxin (Guo et al., 2018; Suneja et al., 1987). Based on these results, a single oral dosage of 2 mg/kg b.w. of Wistar rat in the present study was used to investigate liver injury. A day before intragastrical (i.g.) exposure to T-2 toxin, all animals received fresh water only, without basic feed. Control rats received PBS-DMSO in place of T-2 toxin. All animal work complied with the NIH publication “The Development of Science-Based Guidelines for Laboratory Animal Care” (NRC National Research Council, 2004).

2.4. Cell treatments

To determine the optimal incubation concentration and time for the toxicity of T-2 toxin in BRL cells, 1×10^5 cells/mL were seeded in 96-well plates. The cells were treated of T-2 toxin at different concentrations (0, 2.5, 5, 10, 20, 30, 40, 60 and 80 nM) for 0.5, 1, 2, 4, 8, 12, 24 and 36 h, respectively. After treatment, 20 μL of MTT (0.5 mg/mL) was added to each well and incubated for 4 h. Next, the supernatants of each well were discarded, and 150 μL of DMSO was added to each sample to dissolve the purple formazan crystals. After 10 min, the optical density (OD) was read on a microplate reader (Bio-Tek Instruments, Inc., Winooski, VT, USA). For inhibitor assays, cells were pre-treated with the DNA methylation inhibitor, DAC (5 μM) for 1 h, followed by the addition of T-2 toxin (40 nM) for 12 h. All cell experiments were performed at least in triplicate on three separate occasions.

Table 1
Primers used for RT-PCR analysis.

Gene	Type	Primer sequence (5′to 3′)	Product size (bp)	**Annealing temperature (°C)**
β-actin	Forward	GAGATTACTGCCCTGGCTCCTA	148	55
	Reverse	ACTCATCGTACTCCTGCTTGCTG		
IL-6	Forward	CTGGTCTTCTGGAGTTCCGT	222	55
	Reverse	TCTTGGTCCTTAGCCACTCCT		
IL-1β	Forward	TTGCTTCCAAGCCCTTGACT	236	60
	Reverse	GGTCGTCATCATCCCACGAG		
IL-11	Forward	GCTTCCTGGAGTGCTGACAA	155	55
	Reverse	GTAAGCGACGAAGTAGCCGT		
IL-1α	Forward	GGAGGCCATAGCCCATGATTT	110	56
	Reverse	TGAACTCCTGCTTGACGATCC		
TNF-α	Forward	ACTGAACTTCGGGGTGATCG	153	55
	Reverse	GCTTGGTGGTTTGCTACGAC		
DNMT1	Forward	ACTGTTCCTCCTTCTGCCATC	112	60
	Reverse	CATCGTCCTTAGCGTCGTCG		
DNMT 3A	Forward	CTTGGTGGTTAGGAGGTCGG	85	60
	Reverse	GCCTGTATTCCAGACGGCAC		
DNMT 3B	Forward	GATCAAGCTCACGGCTGTCT	196	60
	Reverse	CTGTTGCTGTTTCGGGTTCG		

Note: The primers were manufactured by Nanjing Genescript Co. Ltd. (Nanjing, PR China). IL-11, interleukin-11; IL-6, interleukin-6; IL-1α, interleukin-1α; TNF-α, tumor necrosis factor alpha; IL-1β, interleukin-1β; and DNMT1, DNA Methyltransferase 1; DNMT3A, DNA Methyltransferase 3A; DNMT3B, DNA Methyltransferase3B.

2.5. Total mRNA isolation and RT-PCR

The mRNA expression of genes related to inflammatory injury and DNA methylation (IL-11, IL-6, IL-1α, IL-1β, TNF-α, DNMT1, and DNMT3A) was measured in rat livers and was determined by real-time quantitative reverse RT-PCR. Total RNA from each liver was isolated using the TRIzol extraction method according to the manufacturer's instructions (Invitrogen Inc., Carlsbad, CA). The quality of RNA was verified by evaluating the optical density at 260 nm and 280 nm. The extracted RNA was reverse-transcribed into cDNA using a PrimeScript RT-PCR kit (TaKara, Dalian, P.R. China) for quantitative PCR.

Primer Express Software was applied to design the rat-specific primers according to the software guidelines (Table 1). Each 25 μL reaction mixture consisted of 12.5 μL of SYBR® Premix Ex Taq™, 1.0 μL of each primer (10 μM), 2.0 μL of cDNA and 8.5 μL of RNase Free H_2O. For all genes, the cycling conditions were as follows: step 1, 30 s at 95 °C; step 2, 45 cycles of 95 °C for 5 s, 50–60 °C for 30 s; step 3, dissociation stage. In this study, the housekeeping gene β-actin was used as an internal calibrator reference gene for expression profiling of genes. Data were analyzed and quantified using the $2^{-\Delta\Delta Ct}$ methods (Liu et al., 2017b).

2.6. Protein extraction and western blot analysis

BRL cells in 6-well plates were incubated with T-2 toxin or co-incubated with inhibitors. After the incubation, the total protein was extracted and analyzed as previously described (Liu et al., 2017b). Briefly, the protein was collected, quantified, and separated by 10% SDS-polyacrylamide gel electrophoresis, and subsequently transferred onto a PVDF membrane (Millipore, Billerica, MA, USA). Membranes were incubated with primary antibodies (diluted according to the manufacturer's instructions) overnight at 4 °C. After washing, blots were incubated for 1 h with the corresponding secondary antibody at a 1:5000 dilution. Immunoreactive bands were detected using the Luminata Classico Western HRP Substrate Kit (Millipore, Bedford, MA, USA), and signal intensity and images were captured with a LAS-4000 luminescent image analyzer (Fujifilm, Tokyo, Japan).

2.7. Histopathological analysis

Histopathological tests were performed using standard laboratory procedures. Control and T-2 toxin-treated animals were sacrificed at specific time points. Liver tissue was dissected from animals, fixed in 10% neutral-buffered paraformaldehyde and paraffin embedded. Routinely, 5 μm or 10 μm sections by microtome and placed onto glass slides for hematoxylin-eosin (HE) staining. Slides were observed under an optical microscope (Olympus BX 41, Japan) for morphological alterations.

2.8. Immunohistochemical assay

Liver tissue was dissected from animals, fixed in 10% neutral-buffered paraformaldehyde and paraffin embedded for slice processing on appropriate glass slides. These were placed into the oven at 58 °C for 10 min, followed by deparaffinization in xylol, rehydration in alcohol at decreasing concentrations, washing in distilled water, and then washing in PBS (0.1 M sodium phosphate buffer, pH 7.2) for 5 min. The endogenous peroxidase was blocked with a 3% hydrogen peroxide solution for 30 min, washing in distilled water, and then washing in PBS for 15 min (3 times, 5 min each). The slides were placed in citrate buffer and subjected to steam heat recovery by maintaining them at 95–100 °C for 30 min, then with natural cooling taken out. The glass slides were then washed with PBS (3 times, 5 min each) and incubated with 5% BSA for 1 h in a moist chamber at 37 °C. After that, the BSA was discarded, followed by overnight incubation with appropriate primary antibodies at 4 °C in a moist chamber. The glass slides were then washed with PBS (3 times, 5 min each) and incubated with the biotinylated secondary antibody for 1 h at 37 °C in the moist chamber. After another wash in PBS (5 times, 5 min each), they were incubated in 0.1% DAB solution (in 3% hydrogen peroxide). The glass slides were counter stained with hematoxylin for 2 min, then washed in running water for 10 min. Finally, the glass slides were washed in distilled water and dehydrated in alcohol (at increasing concentrations), diaphanized in xylol and mounted on Entelan® for optic microscopy examination. Three slides were read for each rat in each group under (400×) magnification and quantitatively measured the average optical density (OD) of each slide with the software Image-Pro Plus 6.0.

2.9. Genome-wide DNA methylation analysis

To test whether methylation of genomic DNA was affected by T-2 toxin, DNA in liver tissue was extracted using a universal genomic DNA kit following treatment with T-2 toxin. A MethylFlash Methylated DNA Quantification Kit was used to detected DNA methylation in the

Table 2
Primers used for Methylation-specific PCR (MSP).

Gene		Type	Primer sequence (5′to 3′)	Product size (bp)	**Annealing temperature (°C)**
IL-11	m	Forward	TTACGAGGGTGATTTTTTTATTTTC	102	55
		Reverse	CCTCGAACCTATATCATCTCTAACG		
	u	Forward	CCCTCAAACCTATATCATCTCTAACA	102	54
		Reverse	TTATGGAGTATTTGTTTTAGTTCGA		
IL-1α	m	Forward	TTATGGAGTATTTGTTTTAGTTCGA	153	52
		Reverse	TAACTTAATCTACCTATTTCTCGCT		
	u	Forward	ATTATGGAGTATTTGTTTTAGTTTGA	153	54
		Reverse	TAACTTAATCTACCTATTTCTCACT		
IL-6	m	Forward	GTTTGATTTAGTTTAGAAGTTTCGG	177	55
		Reverse	AAAAATTTATTACAATCCTTACGTT		
	u	Forward	GTTTGATTTAGTTTAGAAGTTTTGG	177	54
		Reverse	AAAAATTTATTACAATCCTTACATT		
TNF-α	m	Forward	TTGAGATGTGTTGTAATTAAGACGA	146	52
		Reverse	ATAAACTCAACCCTAAAAATTCACG		
	u	Forward	TTGAGATGTGTTGTAATTAAGATGA	146	51
		Reverse	AAACTCAACCCTAAAAATTCACAAA		

m = methylated, u = unmethylated.

Table 3
Primers used for Bisulfite sequencing PCR (BSP).

Gene	**Type**	Primer sequence (5′to 3′)	Product size (bp)	CpG size	Annealing Temperature (°C)
TNF-α BSP	Forward	GAATAGGATTTATTTGAGAGAGGGA	393	6	51
	Reverse	CCTTAAATTAATCTCCCTAACCT			
IL-6 BSP	Forward	TATTTGGAGATAGGTGGATAGAAAAT	279	4	52
	Reverse	CATTTCCAAATCATACAAAAA			
IL-1β BSP	Forward	ATTATAGGTGTGTTTAGGGGA	385	4	52
	Reverse	ACAAACTTATACCTTCTAATAATACCAAAA			
IL-11 BSP1	Forward	TAGGAGGGTTAAATATTTGAGAT	397	5	51
	Reverse	AACCCCTACTCCTACTAAAACCC			
IL-11 BSP2	Forward	TTAGAGGGGTTATTAGGTTGAGG	399	6	52
	Reverse	AAAACATTTCACCAAATATCCCTAA			
IL-1α BSP1	Forward	GATAGTTATATTGGAATTGGAGAG	389	4	52
	Reverse	AAAAAATATAAATTCTTACACAAATCAACA			
IL-1α BSP2	Forward	AGAAATTAAATGGTTAGGTAGTGAT	395	4	52
	Reverse	CAAAAATAAACTAAAACCAAAACTTAAA			

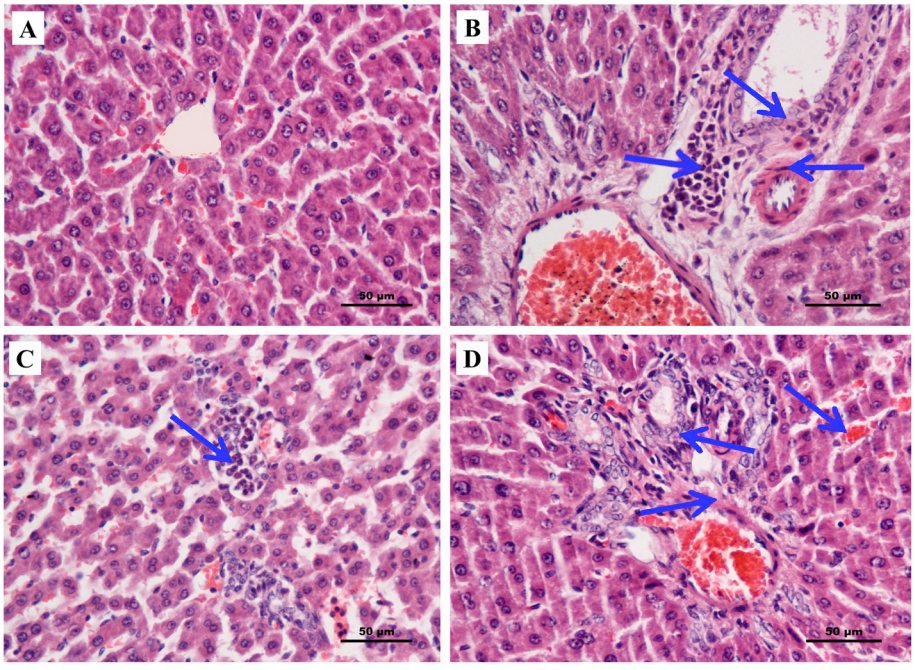

Fig. 1. The selected microphotographs of the liver (400 ×). (A) The liver from the control group. (B) The liver from 1 day after treated with T-2 toxin group. (C) The liver from 3 days after treated with T-2 toxin group. (D) The liver from 7 days after treated with T-2 toxin group. The blue arrow indicates the location of liver injury. (For interpretation of the references to color in this figure legend, the reader is referred to the Web version of this article.)

genome, according to the manufacturer's instructions. Finally, the absorbance (OD) was measured and read with 450 nm within 2–15 min. The following formula was used to calculate 5-mC level: 5-mC = [(Sample OD-ME3 OD) ÷S]/[(ME4 OD-ME3 OD) × 2 ÷ P]; where ME3 = Negative control; ME4 = Positive control; S = Input of DNA sample; P = Quantity of ME4 DNA.

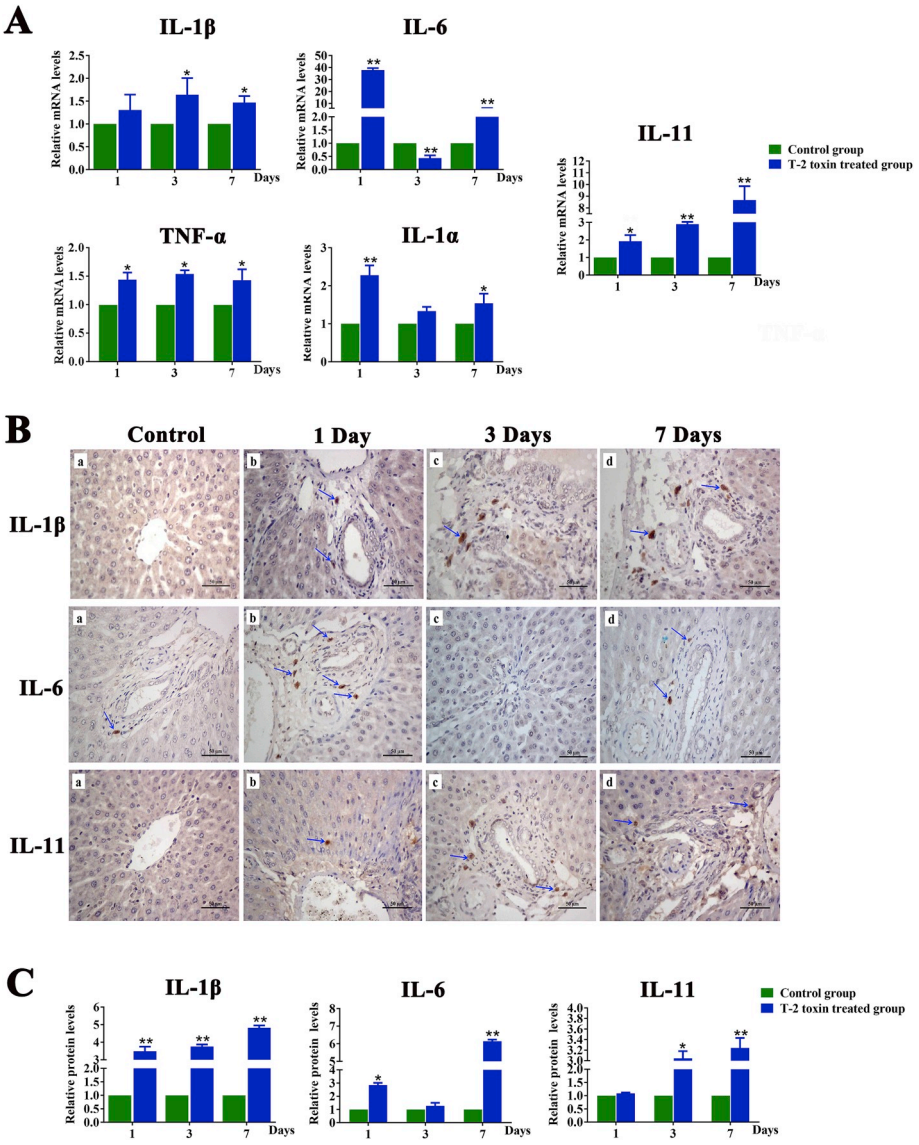

Fig. 2. The relative expression levels of inflammation factors in rat liver. (A) The mRNA expression levels of IL-1β, IL-6, IL-11, TNF-α, and IL-1α detected by RT-PCR. (B–C) The protein expression levels of IL-1β, IL-6, and IL-11 detected by immunohistochemical assays (brown staining is the positive reaction of antibodies for IL-1β, IL-6 and IL-11); a, b, c and d represent the control group, 1-day treatment group, 3-day treatment group and 7-day treatment group, respectively. $*p < 0.05$, $**p < 0.01$, $***p < 0.001$ versus control group. (For interpretation of the references to color in this figure legend, the reader is referred to the Web version of this article.)

2.10. MSP analysis

To determine the methylated DNA in liver tissue, EZ DNA Methylation-Gold Kit was used according to the manufacturer's directions. Methylated and unmethylated primers for IL-11, IL-6, TNF-α, and IL-1α were synthesized by Nanjing Genescript Co. Ltd. (Nanjing, P.R. China) (Table 2). MSP using the following cycle parameters: 95 °C for 5 min, followed by 20, 30 and 40 cycles respectively, at 95 °C for 30 s, 50–60 °C for 30 s and 72 °C for 30 s, and a final extension at 72 °C for 7 min. The PCR product (5 μl) was subjected to electrophoresis on 3% agarose gels and stained with 0.5 μg/ml ethidium bromide. Optical density values were measured using Quantity One 4.6.2 (Bio-Rad Laboratories, Inc., Hercules, CA, USA). The following formulas were used to calculate the results of methylation or unmethylation: methylation rate (%) = $[OD_m]/[OD_{m+}OD_u]$, unmethylation rate (%) = $[OD_u]/[OD_{m+}OD_u]$; where m indicated methylated and u indicated unmethylated.

2.11. Bisulfite sequencing analysis

DNA extracted from BRL cells was treated with bisulfite modification and examined for the methylation status of CpG dinucleotides within the promoter region of the inflammatory factor genes for IL-11, IL-6, IL-1α, TNF-α, and IL-1β. Inflammatory factor gene promoters were amplified from the bisulfite-modified sequence by BSP primers. For the primer amplification system, each 20 μL reaction mixture consisted of 10 μL Zymo Taq™ Premix, 0.5 μL of each primer (10 μM), 2 μL template DNA and 7 μL RNase Free H_2O. For all genes, the cycling conditions were as follows: initial denaturation for 10 min at 95 °C; denaturation at 30 s at 95 °C; annealing at 50–55 °C for 30 s; extending at 72 °C for 30 s; final extension at 72 °C for 7 min. The PCR product was recovered and purified after agarose electrophoresis. The product of PCR was joined to T vector, then cloned and selected blue colonies for sequencing. In the process of cloning, we used water as the negative control and T-vector transformed competent cells as the positive

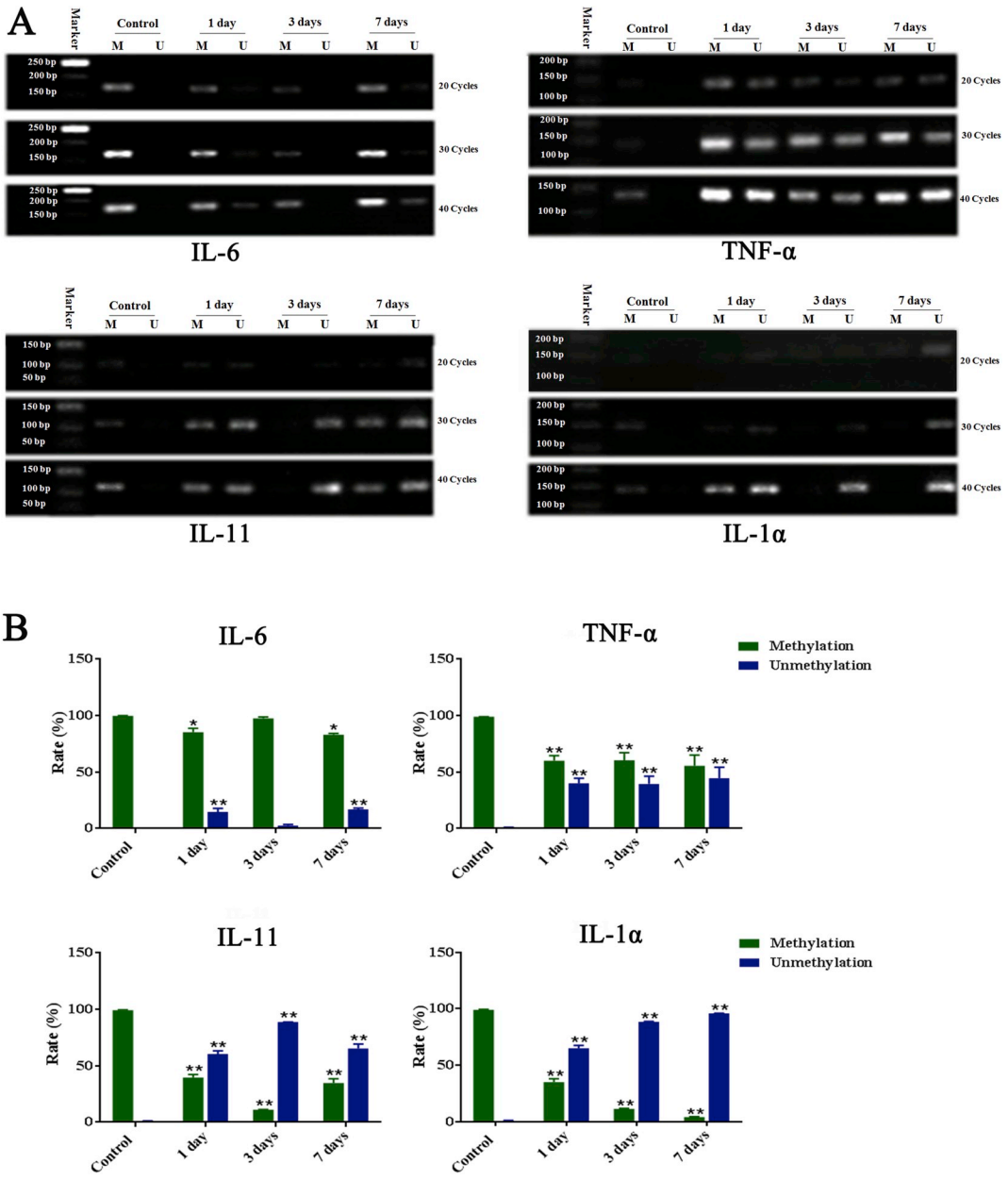

Fig. 3. Genomic DNA extracted from the liver was treated with bisulfite and then subjected to methylation-specific PCR (MSP) using the methylated DNA (m)-and unmethylated DNA (u)-specific primer sets. In the figure, M represents methylation, U represents unmethylation. $*p < 0.05$, $**p < 0.01$, $***p < 0.001$ versus control group.

control. We aligned, visualized, and quantified bisulfite sequence data for CpG methylation analysis by Quantitative tool for methylation analysis (QUMA) software. The sequences of primers are shown in Table 3.

2.12. Nuclear morphology and cell apoptosis analysis

BRL cells (1×10^5/mL) were seeded in a 12-well plate and cell growth reached approximately 80–90%. Cells were incubated with T-2 toxin (40 nM) and DAC (5 μM) for 12 h. After treatment, cells were washed twice with PBS. DAPI staining solution was added to each hole and incubated for 10 min in the dark. Nuclear changes were observed under a fluorescence microscope (excitation wavelength 364 nm and emission wavelength 454 nm).

Cell apoptosis was measured by Annexin V-FITC Apoptosis Detection Kit, as described in our previous study (Liu et al., 2017a). BRL cells were incubated with T-2 toxin (40 nM) and DAC (5 μM) for 12 h. After treatment, cells were washed twice with PBS and incubated in 300 μL binding buffer containing 3 μL annexin V-FITC stain and 3 μL PI in the dark for 15 min at room temperature. The stained samples (containing 200, 000 cells/sample) were then analyzed on a flow cytometer within 1 h, following the manufacturer's protocol (CyAn ADP, Beckman, Irvine, CA, USA).

2.13. Statistical analysis

The statistical analysis was performed using SPSS 18.0 for Windows. The Mann–Whitney non-parametric test was used for the BSP data analysis (Elika et al., 2009; Yu et al., 2019). The results are expressed as mean ± SD. Group differences were assessed using one-way analysis of

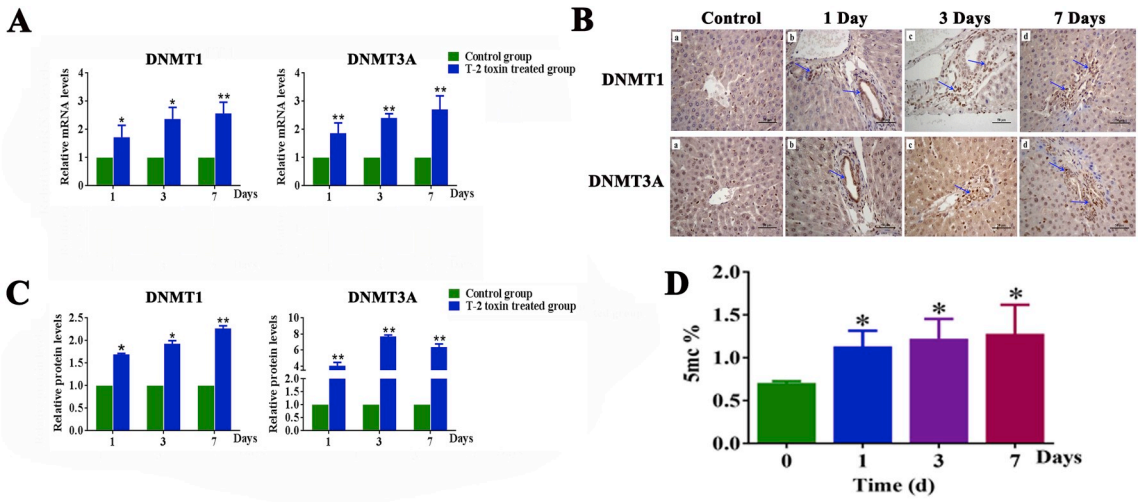

Fig. 4. The relative expression of DNA methyltransferases and the 5-mC level of genomic genes in the rat liver. (A) The mRNA levels of DNMT1 and DNMT3A detected by RT-PCR. (B–C) The protein expression levels of DNMT1 and DNMT3A detected by immunohistochemical assays (brown staining is the positive reaction of antibodies for DNMT1 and DNMT3A); a, b, c, and d represent the control group, 1-day treatment group, 3-day treatment group and 7-day treatment group, respectively. (D) The 5-mC level of genomic genes was assessed using the MethylFlash Methylated DNA Quantification Kit (colorimetric). $*p < 0.05$, $**p < 0.01$, $***p < 0.001$ versus control group. (For interpretation of the references to color in this figure legend, the reader is referred to the Web version of this article.)

variance (ANOVA), followed by the least significant differences (LSD) tests. Values for which $p < 0.05$ denoted significant differences from the control.

3. Results

3.1. Clinical observations after T-2 toxin exposure

Before the start of the experiment, the rats were fed with their standard feeds. However, one day after they had been administered T-2 toxin, rats in the experimental group began to exhibit poor mental states such as slow action. During the 5 days of T-2 toxin administration, the animal's food intake decreased. From the sixth day of the experimental condition, poor symptoms improved and had nearly recovered completely by the end of the experimental protocol. These clinical changes suggest that T-2 toxin may cause changes in the diet and mental status in rats.

3.2. Histological evaluation in rat liver

As shown in Fig. 1, the significant histopathological changes in liver tissue were observed in T-2 toxin-treated rats. In the liver of the control animals, liver cells and hepatic sinusoids were radically arranged around the central vein, and the liver cells were more deformed with intact structures and large, round nuclei (Fig. 1A). Compared to the control group, results from rat livers treated with T-2 toxin for 1 day revealed that the contour of the liver cells was not clear, and some central lobes of hepatic lobules were denatured (granule sense). Occasionally, neutrophil infiltration in the portal area and slight proliferation of central venous peripheral bile duct epithelial cells were observed (Fig. 1B). After treatment with T-2 toxin for 3 days, the nuclei of hepatocytes were different in size, indicating proliferation, and lymphocytes and neutrophils are aggregated in hepatic lobules (Fig. 1C). In rats treated with T-2 toxin for 7 days, bile duct epithelial cells in the tubular area showed slight proliferation, and inflammatory lymphocytes were aggregated; in the liver, levels of hyper binuclear hepatocytes were increased and slight bleeding occurred (Fig. 1D). These results indicate that hepatocytes are damaged after acute exposure to T-2 toxin, and the resulted proliferation is probably inflammatory hyperplasia.

3.3. T-2 toxin promotes the production of pro-inflammatory cytokines in rat liver

To determine whether T-2 toxin exposure causes hepatic inflammation in rats, the mRNA and protein expression of inflammatory factors was examined. As shown in Fig. 2, the mRNA expression levels of IL-1β were significantly higher after T-2 toxin exposure for 3 or 7 days ($p < 0.05$), and the mRNA expression levels of IL-1α, and IL-6 were higher after exposure for 1 day or 7 days ($p < 0.05$), compared to the control group. However, the mRNA expression levels of IL-6 were significantly lower after T-2 toxin exposure for 3 days ($p < 0.01$). The expression level of TNF-α significantly increased after T-2 exposure for 1, 3, and 7 days ($p < 0.05$). The protein levels of IL-1β, IL-6, and IL-11 in the liver were also assessed by immunohistochemical staining, which showed that the levels of IL-1β and IL-6 were consistent with the trend of the corresponding mRNA expression. The protein levels of IL-11 increased after T-2 toxin exposure for 3 days ($p < 0.05$) and 7 days ($p < 0.01$). Thus, T-2 toxin exposure caused an inflammatory response *in vivo* by accumulating pro-inflammatory factors.

3.4. Analysis of methylation levels of CpG sites in inflammatory cytokine promoter regions in rat liver under T-2 toxin

The present study used MSP to measure the methylation levels of CpG sites in IL-11, IL-6, IL-1α, and TNF-α genes promoter region (Fig. 3). In T-2 exposure groups, the unmethylation levels of IL-11, IL-1α, and TNF-α promoter regions significantly increased compared with the control ($p < 0.01$), inducing the expression of these inflammatory factors. Additionally, the unmethylation level of IL-6 was significantly higher after T-2 toxin exposure for 1 and 7 days. Using PROMO online software, the CpG sites of IL-6, IL-11, IL-1α, and TNF-α promoter regions analyzed by MSP method were relevant for transcription factors (TFs) binding, which was shown in the Supplementary data. These results indicated that DNA demethylation facilitated the binding of inflammatory gene promoters and TFs, thereby leading to the expression of inflammatory factors in rat liver treated with T-2 toxin.

3.5. T-2 toxin causes abnormal expression of DNA methyltransferases and affects the genomic 5-mC levels in rat livers

To investigate the role of DNA methylation in the inflammatory

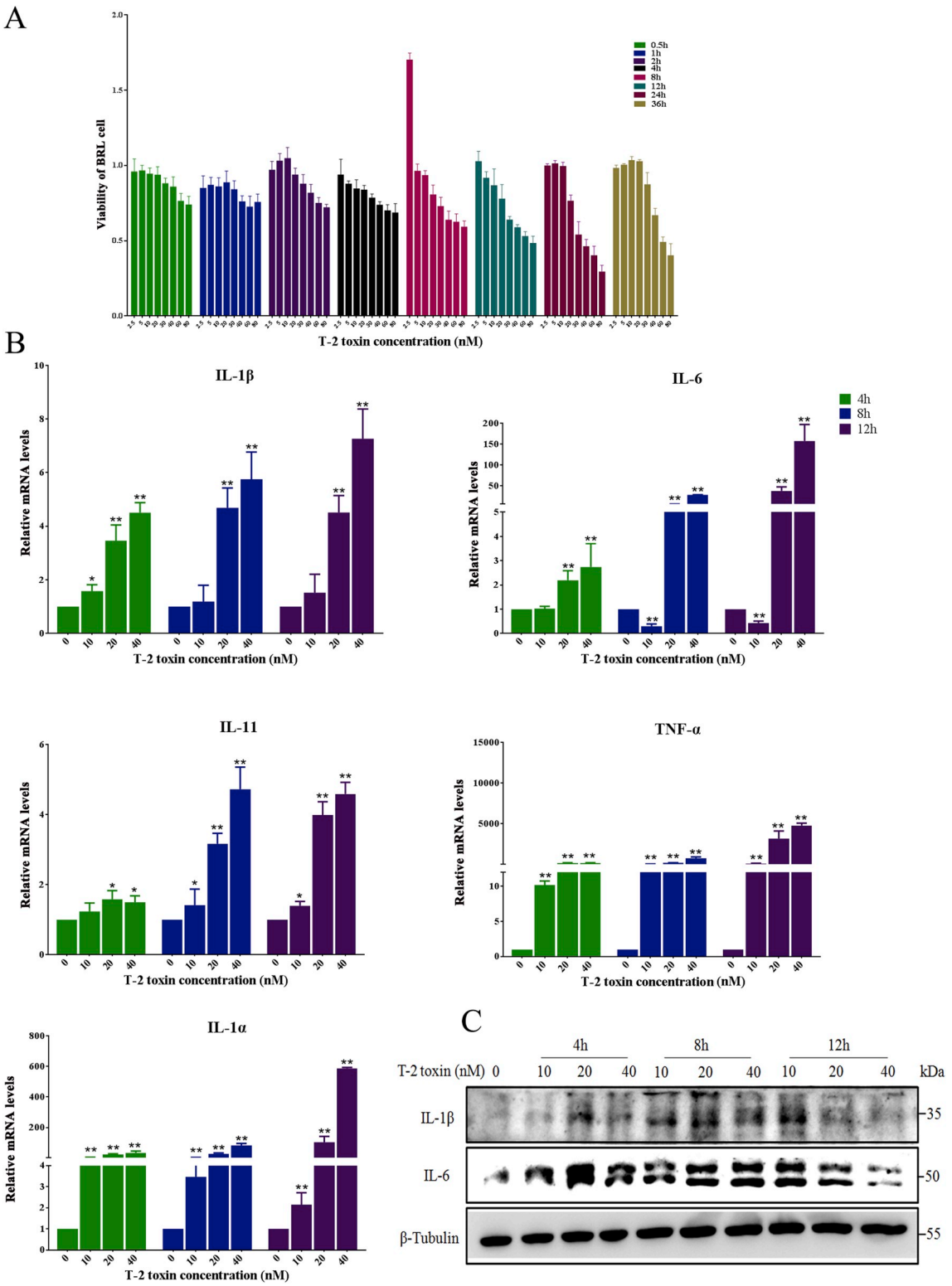

Fig. 5. T-2 toxin-induced cytotoxicity in BRL cells exhibited by reduced cell viability and increased inflammatory cytokines. (A) BRL cells were treated with T-2 toxin (0, 2.5, 5, 10, 20, 30, 40, 60 and 80 nM) for 0.5, 1, 2, 4, 8, 12, 24 and 36 h and cell viability was assessed by an MTT cell proliferation assay. (B) After BRL cells were treated with T-2 toxin (10, 20 and 40 nM) for 4, 8 and 12 h, respectively, the mRNA levels of IL-1β, IL-6, IL-11, TNF-α, and IL-1α were detected by RT-PCR. (C) BRL cells were exposure to T-2 toxin (10, 20, and 40 nM) for 4, 8, and 12 h, and the protein levels of IL-1β and IL-6 were assessed by Western blot. $^{*}p < 0.05$, $^{**}p < 0.01$, $^{***}p < 0.001$ versus control group.

toxicity of T-2 toxin exposure, the expression of DNMT1 and DNMT3A was examined. Our results demonstrated that mRNA expression levels of DNMT1 significantly increased after exposure to T-2 toxin ($p < 0.05$), and DNMT3A levels significantly increased after exposure for 3 days ($p < 0.05$) and 7 days ($p < 0.01$; Fig. 4A). The protein levels of DNMT1 and DNMT3A in the liver were also assessed by immunohistochemical staining, the positive result for which indicated that DNMT1 and DNMT3A significantly increased after T-2 toxin exposure

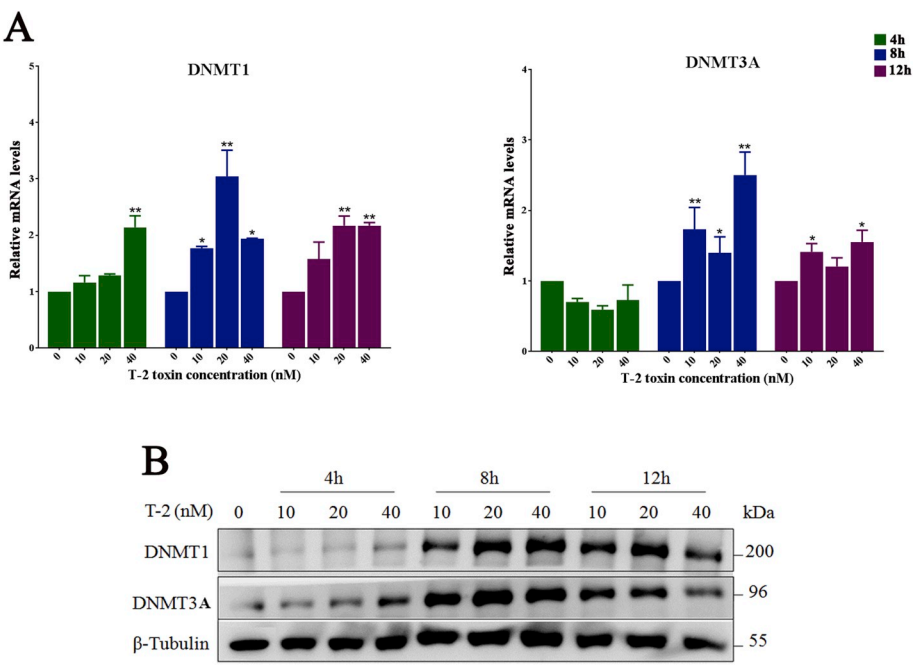

Fig. 6. The effect of T-2 toxin on the expression of DNA methyltransferase. (A) After BRL cells were treated with T-2 toxin (10, 20 and 40 nM) for 4, 8, and 12 h, the mRNA levels of DNMT1and DNMT3A were detected by RT-PCR. (B) The protein levels of DNMT1 and DNMT3A were assessed by Western blot. $^{*}p < 0.05$, $^{**}p < 0.01$, $^{***}p < 0.001$ versus control group.

for 1, 3, 7 days (Fig. 4B and C). Thus, DNA methylation might be an important mechanism for hepatotoxicity induced by T-2 toxin in rats. Furthermore, we tested whether T-2 toxin affects the genomic DNA methylation levels in rat livers. Our results revealed that 5-mC global levels were significantly higher in livers treated with T-2 toxin than in the controls ($p < 0.05$; Fig. 4D).

3.6. Effects of T-2 toxin in BRL cells by MTT

The cytotoxicity of T-2 toxin in BRL cells was determined by the MTT assay (Liu et al., 2017a). EC_{50} was a standardized endpoint for the cytotoxicity study. In this study, the results of the MTT assay displayed a dose-and time-dependent decrease in cell viability that was induced by T-2 toxin in rat liver BRL cells (Fig. 5A). Considering the state of the BRL cells and the EC_{50} results of the MTT assay, the levels of 10, 20 and 40 nM for 4, 8 and 12 h of exposure time was selected for the subsequent studies.

3.7. T-2 toxin induced high expression of inflammatory cytokines and DNA methyltransferases in BRL cells

In vitro studies showed that T-2 toxin significantly elevated the expression of inflammatory factors in BRL cells. As shown in Fig. 5B, the mRNA expression of IL-1β, IL-6, IL-11, TNF-α and IL-1α induced by T-2 toxin significantly increased after exposure at doses of 10, 20 and 40 nM for 4, 8 and 12 h, respectively. This process was dose-dependent, and the highest mRNA levels of these genes were observed at 40 nM for 12 h. IL-1β and IL-6 are the most important inflammatory factors in the process of an inflammatory reaction; they are also the main inflammatory targets induced by T-2 toxin (Liu et al., 2017a, 2017b). After the cells were incubated with different concentrations of T-2 toxin (10, 20 and 40 nM) for 4, 8 and 12 h, IL-1β and IL-6 protein expression was consistent with mRNA expression (Fig. 5C). These results illustrate that the large production of inflammatory factors is a mechanism of cytotoxicity induced by T-2 toxin, which is in agreement with the results of previous studies in other cells (Liu et al., 2017a).

Additionally, the results in Fig. 6A suggested that the mRNA levels of DNMT1 and DNMT3A have varying degrees of elevation after BRL cells were treated with T-2 toxin (10, 20 and 40 nM) for 8 and 12 h. The relative protein levels of DNMT1 and DNMT3A also elevated in BRL cells treated with the same concentrations of T-2 toxin (Fig. 6B). These results indicated that T-2 toxin increased the expression of DNA methylationtransferases, leading to abnormal methylation of genes, such as those inflammatory factors or genes associated with inflammation.

3.8. Effect of T-2 toxin on DNA methylation and expression of inflammatory cytokines in vitro

To further determine whether the high expression of inflammatory factors is related to DNA methylation after exposure to T-2 toxin in BRL cells, the effect of DAC, a demethylating agent, was examined and bisulfite sequencing (BSP) was applied. Treatment with DAC combined with T-2 toxin significantly increased the mRNA levels of IL-1β, IL-6, IL-11, and TNF-α compared with the T-2 toxin group, while, expression of IL-1α was not increased significantly (Fig. 7A). We also detected the protein levels of IL-6 and IL-1β, and the result was consistent with their mRNA expression (Fig. 7C). Furthermore, the treatment of DAC combined with T-2 toxin significantly reduced cell viability (Fig. 7B), which may be related to the increase of inflammatory factors. Importantly, T-2 toxin led to the significant hypomethylation of TNF-α promoter CpG sites (−1290), and IL-11 promoter CpG sites (−424, −1602, −1644, −1659), thus promoting the expression of these two genes (Fig. 8). Moreover, in the DAC combined with T-2 toxin group, the methylation levels of TNF-α promoter CpG site (−1290) and IL-11 gene promoter CpG site (−678) were markedly decreased compared with T-2 toxin alone. Using PROMO online software, the CpG sites of IL-11 and TNF-α promoter regions analyzed by BSP were related to TFs binding, which was shown in the Supplementary data. *In vitro* results further demonstrated that T-2 induced DNA demethylation of IL-11 and TNF-α promoter, which facilitates the binding of transcription factors to promoter and up-regulates the expression of IL-11 and TNF-α.

In addition, T-2 toxin did not affect the CpG methylation level of IL-6, IL-1β and IL-1α *in vitro*. Notably, although the CpG methylation level of IL-6 and IL-1β promoter region CpG sites remained unchanged in all groups, the expression of these genes significantly increased, indicating DNA demethylation may induce the expression of IL-6 and IL-1β by affecting other genes or the inflammatory signalling pathways.

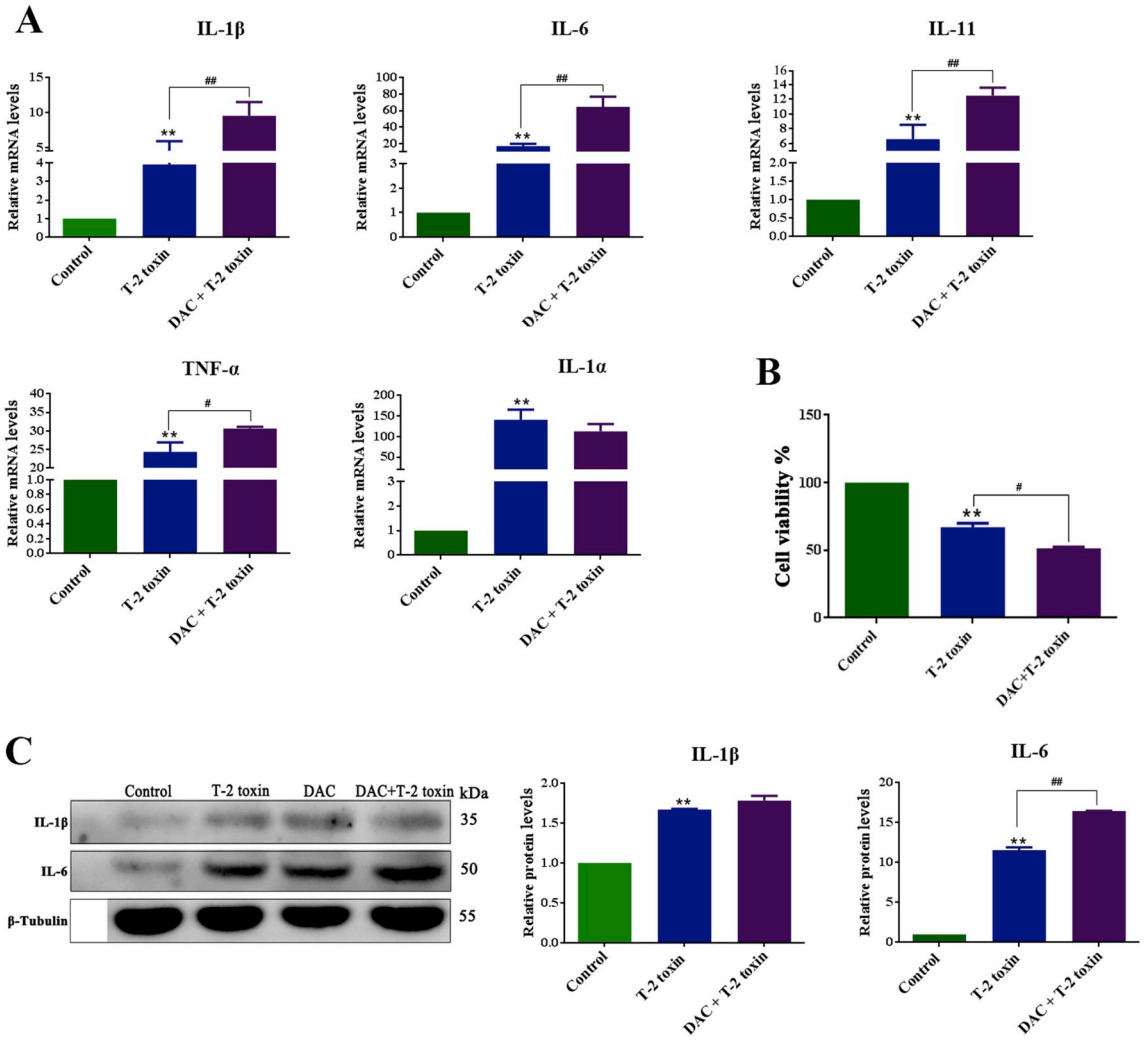

Fig. 7. The effect of DAC on the expression of inflammatory factors. After BRL cells were either left untreated or pre-treated with DAC (5 μM) for 1 h, followed by the addition of T-2 toxin (40 nM) for 12 h, (A) the gene expression of IL-1β, IL-11, IL-6, TNF-α, and IL-1α was assessed by RT-PCR; (B) cell viability was detected by MTT cell proliferation assay; and (C) the protein expression of IL-1β and IL-6 was assessed by Western blot. $^{*}p < 0.05$, $^{**}p < 0.01$ versus control group, $^{\#}p < 0.05$, $^{\#\#}p < 0.01$ versus T-2 toxin group.

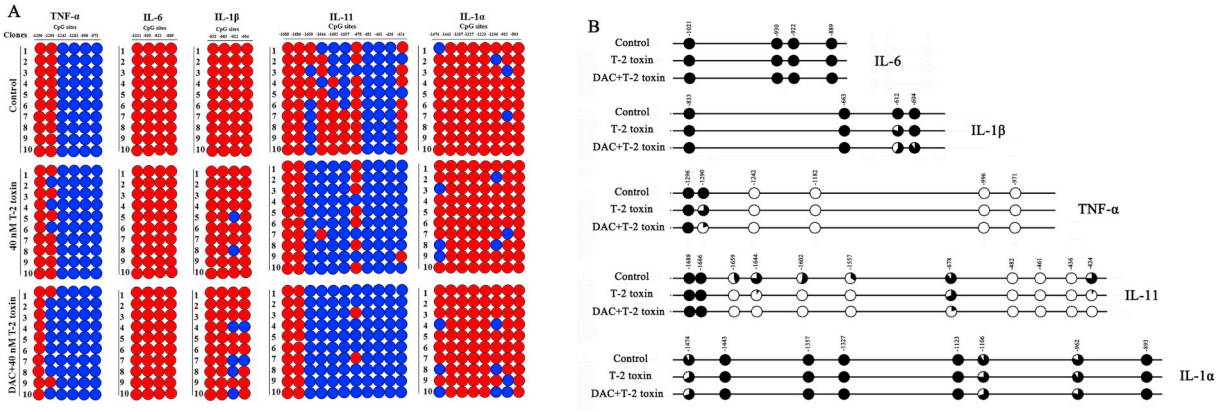

Fig. 8. The methylation levels in the promoter regions of inflammatory factors (TNF-α, IL-11, IL-1β, IL-6, IL-1α) was detected by BSP, which indicates bisulfite sequencing by PCR; the red dots represent the CpG sites of methylation, and the blue dots represent the unmethylated CpG sites (A); the whole circle represents a CpG site, the black area in the circle represents methylation, and the white area represents unmethylation (B). (For interpretation of the references to color in this figure legend, the reader is referred to the Web version of this article.)

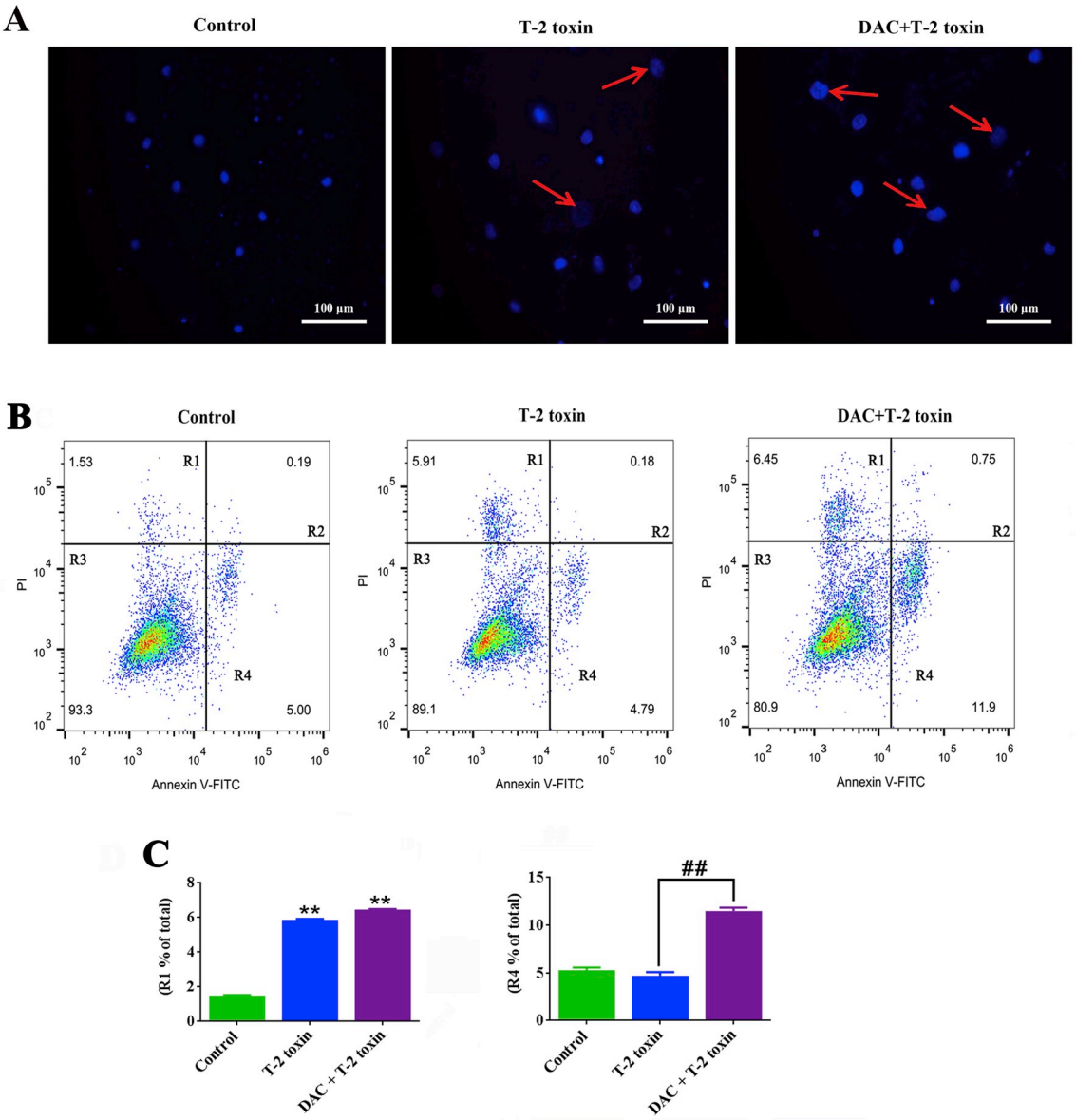

Fig. 9. The effect of T-2 toxin or DAC + T-2 toxin on cell apoptosis. After BRL cells were either left untreated or pre-treated with DAC (5 μM) for 1 h, followed by the addition of T-2 toxin (40 nM) for 12 h; (A) the morphological changes were detected by fluorescence microscopy, with DAPI stain to show the nuclei; (B) the cells were analysed by flow cytometry; and (C) the death and early apoptosis rates of BRL cells were determined. $^{*}p < 0.05$, $^{**}p < 0.01$ versus control group, $^{\#}p < 0.05$, $^{\#\#}p < 0.01$ versus T-2 toxin group.

Note: The red arrow indicates the expansion of the nucleus as compared with the control group (A). R1 phase: necrotic cell; R2 phase: terminal apoptosis cell; R3 phase: live cell; R4 phase: early apoptosis cell (B).

3.9. DNA demethylation mediates BRL cell damage induced by T-2 toxin

As shown in Fig. 9A, after treated with T-2 toxin (40 nM) for 12 h, DAPI staining exposed that T-2 toxin caused nuclear enlargement and chromatin loosening compared with the control group. The results indicate that T-2 toxin may cause cell necrosis. In BRL cells treated for 12 h with DAC combined with T-2 toxin, DAPI staining showed that cell nucleation was larger, and chromatin was loose compared with the T-2 toxin group. Flow cytometry using annexin V-FITC/PI apoptosis detection revealed that the necrosis rate of BRL cells was higher in the T-2 toxin group (Fig. 9B). The early apoptosis cell proportion in R4 phase after exposure to DAC combined with T-2 toxin was significantly higher compared to the T-2 toxin group ($p < 0.05$; Fig. 9B and C). Taken together, we found that T-2 toxin might promote the production of inflammatory factors directly or indirectly through DNA methylation, leading to cell necrosis and cell apoptosis.

4. Discussion

The contamination of T-2 toxin is widespread, and its hepatotoxicity has attracted increasing amounts of attention (Gan et al., 2018; Shinozuka et al., 2009). This study revealed for the first time that pro-inflammatory cytokines and DNA methylation could significantly trigger T-2 toxin hepatotoxicity. T-2 toxin increased the expression of pro-inflammatory cytokines IL-1β, IL-6, IL-11, IL-1α, and TNF-α, those are associated with DNA methylation, causing severe liver injury both *in vivo* and *in vitro*.

The liver is an important target organ of T-2 toxin (Shinozuka et al., 2009; Smith et al., 2017). For instance, T-2 toxin markedly stimulated lipid peroxidation, specifically in the livers of rats and decreasing the amount of cytochrome P-450 of basophilic masses in hepatocytes (Tsuchida et al., 1984). A single dose of T-2 toxin enhanced conjugated diene formation in rat livers, which was also related to lipid

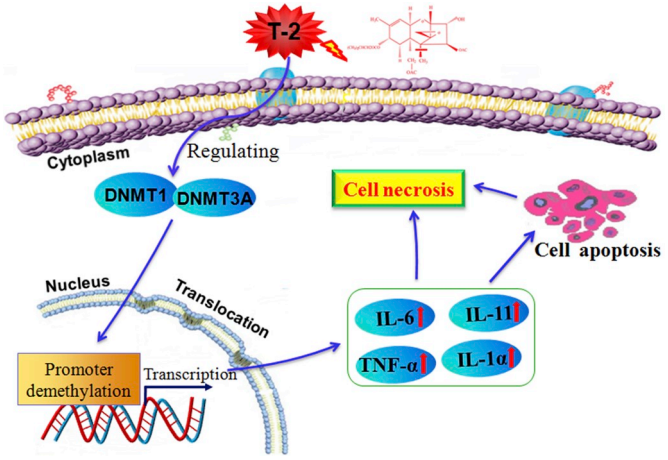

Fig. 10. A mechanism of T-2 toxin inducing inflammatory cytokines via DNA demethylation. T-2 toxin could regulate the expression of DNMT1 and DNMT3A, thereby disrupting the methylation of gene promoter region, such as demethylation of inflammatory cytokine promoter region, which leads to the high expression of inflammatory factors and ultimately leads to apoptosis or necrosis.

peroxidation (Chang et al., 1988). Further, high doses of T-2 toxin are known to decrease protein synthesis and mono-oxygenase activities in the rat liver (Guerre et al., 2000). Previous studies mainly focused on oxidative stress, lipid peroxidation and apoptosis to explore the liver injury caused by T-2 toxin (Sehata et al., 2005). However, the role of inflammation in the hepatotoxicity related to T-2 toxin was unclear. This study showed that T-2 toxin caused infiltration of neutrophils and lymphocytes in the rat liver portal area, and liver cells exhibited inflammatory hyperplasia, which were symptoms of inflammatory toxicity caused by T-2 toxin (Fig. 1). Moreover, T-2 toxin-induced an increase in the expression of pro-inflammatory cytokines (IL-1β, IL-6, IL-11, IL-1α, and TNF-α), which can lead to liver injury (Meszaros et al., 2017). Taken together, these results indicate the production of pro-inflammatory cytokines is a critical mechanism of T-2 toxin-mediated liver injury.

Importantly, this study revealed that T-2 toxin up-regulated the expression of pro-inflammatory cytokines through DNA demethylation, resulting in cell damage. Although there are many inflammatory studies of T-2 toxin (Liu et al., 2017b; Zhou et al., 2014), but very few studies investigated the role of DNA methylation in T-2 toxin-induced inflammation. Herein, our *in vivo* studies showed that demethylation of IL-6, IL-11, IL-1α, and TNF-α gene promoter region were observed in rat liver after administration of T-2 toxin. It might cause TFs (Pax-6, DSXF, DSXM, MYB2, TAF; AP-1, c-Fos; Pax-6, Pax-8, ZF5, E2F-1, Pax-4a; c-Rel, STAT5B, Pax-6, Pax-2a, HSF1) (shown in Supplementary data) to bind to IL-6, IL-11, IL-1α and TNF-α promoter regions, respectively, and promotes the expression of inflammatory genes. *In vitro* study, the methylation level of the TNF-α gene dropped substantially at one CpG site (−1290) in T-2 toxin-exposed BRL cells, and sequences containing this site might be the binding site of TFs such as CREB, Jun-B, c-Jun, Pax-2a (shown in Supplementary data), regulating TNF-α expression. These results suggested that the demethylation levels at CpG sites enhanced the transcription activity of the TNF-α gene to some extent (Kaut et al., 2014; Zhang et al., 2016). Administration of T-2 toxin combined with DAC led to slightly lower TNF-α gene methylation levels at the CpG site compared to T-2 toxin alone (Fig. 8), which is consistent with results where the DAC and T-2 toxin combination produced an extremely significant increase in expression of TNF-α (Fig. 7A) and the rate of cell death (Fig. 9). Therefore, T-2 toxin can promote TNF-α expression by hypomethylation of TNF-α promoter.

Additionally, our results from *in vitro* studies demonstrated that T-2 toxin promoted high expression levels of the IL-11 gene by promoter demethylation at six CpG sites, and sequences containing these CpG sites might be the binding site of TFs such as CREB Zic1 and Zic3 (shown in Supplementary data), indicating demethylation of IL-11 promoter region induced the binding of TFs and promoters, and thus promotes the expression of IL-11. Treatment with DAC and T-2 toxin combined significantly promoted the production of IL-11, which in turn suggests that DNA methylation can mediate IL-11 expression. Exploring the expression mechanism of TNF-α and IL-11 from the perspective of DNA methylation will provide a new therapeutic strategy for its related diseases and T-2 toxin toxicity.

Interestingly, our study showed that DNA demethylation might induce the expression of IL-6 and IL-1β under T-2 toxin treatment. There are differences in gene methylation under different treatments in various models (De Smedt et al., 2018). For instance, in LPS-stimulated broiler peripheral blood mononuclear cells, methionine increased the methylation of 191 CpG sites of IL-6 promoter region, and thus decreased the IL-6 expression level (Shen et al., 2017). However, LPS decreased methylation level of specific CpG sites at the IL-6 promoter in bovine endometrial cells (at 366 and 660 sites) after 24 h and increased IL-6 mRNA expression (Wang et al., 2018a). In CD34+/CD38-acute myeloid leukemia (AML) cells from patients, methylation-specific PCR found that IL-1β gene expression was silenced by hypermethylation of the promoter region (Yang et al., 2013); however, LPS decreased the methylation level of the IL-1β gene promoter and increased intracellular IL-1β production in aged mice (Matt et al., 2016). Additionally, current studies have shown that the expression of IL-6 and IL-1β is closely related to non-CpG methylation (Dinicola et al., 2017; Fuso et al., 2016; Nicolia et al., 2017). In our *in vitro* study, there was no significant change in the CpG methylation level of IL-6 and IL-1β promoters in any treatment groups, which is consistent with the results of exposure to T-2 toxin *in vivo* for 3 days. Surprisingly, administration of DAC combined with T-2 toxin led to high expression of IL-6 and IL-1β compared with T-2 toxin alone (Fig. 7). We speculate that the non-CpG demethylation (CpC, CpT, CpA, etc) of IL-6 and IL-1β promoters or other genes regulated by DNA demethylation may induce the expression of IL-6 and IL-1β genes under T-2 toxin treatment (Dinicola et al., 2017; Yuan et al., 2016; Zhang et al., 2018b).

Very few studies revealed that DNA methyltransferases could mediate trichothecenes-induced toxicity. A recent study showed that deoxynivalenol exposure altered DNMT3A mRNA levels, thus increasing DNA methylation levels in porcine oocytes (Han et al., 2016). In our study, T-2 toxin increased the expressions of DNMT1 and DNMT3A in rat livers (Fig. 4A). These genes were mainly concentrated in the proliferative sites and inflammatory cell infiltrates in the lobular duct of the liver (Fig. 4B), indicating that DNA methyltransferase is a potential novel inducible factor of T-2 toxin inflammatory toxicity (Nakamura et al., 2017). Meanwhile, T-2 toxin increased the global levels of 5-mC in rat livers (Fig. 4D), which positively correlated with increased expression of DNA methyltransferase (Page et al., 2016). These results suggest that the abnormal expression of DNA methyltransferases is closely related to T-2 toxin-induced liver inflammatory injury. T-2 toxin-induced increase of the whole 5-mC gene may be a 'protective stress mechanism', considering that DAC can decrease the level of 5-mC (Shakya et al., 2013), and the treatment of DAC combined with T-2 toxin aggrandized the degree of cell damage with the higher rate of cell apoptosis and death compared to T-2 toxin alone (Fig. 9).

In conclusion, exposure to T-2 toxin resulted in basic lesions of liver cell degeneration, necrosis, inflammatory cell infiltration, and liver cell proliferation, as well as the expression of pro-inflammatory cytokines, where DNA unmethylation mediates the high expression of inflammatory cytokines (Fig. 10). Additionally, T-2 toxin may also regulate DNMTs, and thus disrupts the methylation level of inflammatory genes (Lu et al., 2019). However, the conclusion does not provide a possible molecular mechanism for the epigenetic effect of T-2 toxin. We speculate that T-2 toxin-induced inflammatory-related transcription factors, such as nuclear factor-kappa B (NF-κB) (Bhatt and Ghosh, 2014;

Liu et al., 2017a) are responsible for demethylation of the promoter of the inflammatory genes (Pacis et al., 2019; Wu and Zhang, 2017). Further studies to prove the above hypothesis are still warranted.

Conflicts of interest

The authors declare that they have no conflict of interest.

Acknowledgments

This work was supported by the National Natural Science Foundation of China (grant nos. 31572575 and 31602114) and by the Fundamental Research Funds for the Central Universities (2662016PY115), and University of Hradec Kralove (Faculty of Science, VT2019-2021).

Appendix A. Supplementary data

Supplementary data to this article can be found online at https://doi.org/10.1016/j.fct.2019.110661.

Declaration of interests

The authors declare that they have no known competing financial interestsor personal relationships that could have appeared to influence the work reported in this paper.

References

Arroyo-Jousse, V., Garcia-Diaz, D.F., Codner, E., Perez-Bravo, F., 2016. Epigenetics in type 1 diabetes: TNFa gene promoter methylation status in Chilean patients with type 1 diabetes mellitus. Br. J. Nutr. 116, 1861–1868.

Bhatt, D., Ghosh, S., 2014. Regulation of the NF-kappaB-Mediated transcription of inflammatory genes. Front. Immunol. 5, 71.

Chang, I.M., Mar, W.C., 1988. Effect of T-2 toxin on lipid peroxidation in rats: elevation of conjugated diene formation. Toxicol. Lett. 40, 275–280.

Cheng, C., Huang, C., Ma, T.T., Bian, E.B., He, Y., Zhang, L., Li, J., 2014. SOCS1 hypermethylation mediated by DNMT1 is associated with lipopolysaccharide-induced inflammatory cytokines in macrophages. Toxicol. Lett. 225, 488–497.

De Smedt, E., Maes, K., Verhulst, S., Lui, H., Kassambara, A., Maes, A., Robert, N., Heirman, C., Cakana, A., Hose, D., Breckpot, K., van Grunsven, L.A., De Veirman, K., Menu, E., Vanderkerken, K., Moreaux, J., De Bruyne, E., 2018. Loss of RASSF4 expression in multiple myeloma promotes RAS-driven malignant progression. Cancer Res. 78, 1155–1168.

Deng, Y.J., Wang, Y.L., Sun, L.J., Lu, P.L., Wang, R.D., Ye, L., Xu, D.F., Ye, R.Y., Liu, Y., Bi, S.Y., et al., 2018. Biotransformation enzyme activities and phase I metabolites analysis in Litopenaeus vannamei following intramuscular administration of T-2 toxin. Drug Chem. Toxicol. 41, 113–122.

Dinicola, S., Proietti, S., Cucina, A., Bizzarri, M., Fuso, A., 2017. Alpha-lipoic acid downregulates IL-1b and IL-6 by DNA hypermethylation in SK-N-be neuroblastoma cells. Antioxidants 6, 74.

Elika, M., Petra, K., Bernhard, D., Andrea, H., Rasoul, A.K., Bernard, J., Mullis, P.E., Frey, B.M., Flück, C.E., 2009. Role of DNA methylation in the tissue-specific expression of the CYP17A1 gene for steroidogenesis in rodents. J. Endocrinol. 202, 99.

Fairhurst, S., Marrs, T.C., Parker, H.C., Scawin, J.W., Swanston, D.W., 1987. Acute toxicity of T2-toxin in rats, mice, Guinea-pigs, and pigeons. Toxicology 43, 31–49.

Fuso, A., Iyer, A.M., van Scheppingen, J., Maccarrone, M., Scholl, T., Hainfellner, J.A., Feucht, M., Jansen, F.E., Spliet, W.G., Krsek, P., Zamecnik, J., Muhlebner, A., Aronica, E., 2016. Promoter-specific hypomethylation correlates with IL-1 beta overexpression in tuberous sclerosis complex (TSC). J. Mol. Neurosci. 59, 464–470.

Gan, F., Yang, Y.L., Chen, Y., Che, C.P., Pan, C.L., Huang, K.H., 2018. Bush sophora root polysaccharide could help prevent aflatoxin B1-induced hepatotoxicity in the primary chicken hepatocytes. Toxicon 150, 180–187.

Garrido, C.E., Gonzalez, H.H., Salas, M.P., Resnik, S.L., Pacin, A.M., 2013. Mycoflora and mycotoxin contamination of roundup ready soybean harvested in the pampean region, Argentina. Mycotoxin Res. 29, 147–157.

Guerre, P., Eeckhoutte, C., Burgat, V., Galtier, P., 2000. The effects of T-2 toxin exposure on liver drug metabolizing enzymes in rabbit. Food Addit. Contam. A. 17, 1019–1026.

Guo, P., Liu, A.M., Huang, D.Y., Wu, Q.H., Fatima, Z., Tao, Y.F., Cheng, G.Y., Wang, X., Yuan, Z.H., 2018. Brain damage and neurological symptoms induced by T-2 toxin in rat brain. Toxicol. Lett. 286, 96–107.

Han, J., Wang, Q.C., Zhu, C.C., Liu, J., Zhang, Y., Cui, X.S., Kim, N.H., Sun, S.C., 2016. Deoxynivalenol exposure induces autophagy/apoptosis and epigenetic modification changes during porcine oocyte maturation. Toxicol. Appl. Pharmacol. 300, 70–76.

Hjelkrem, A.G.R., Aamot, H.U., Brodal, G., Strand, E.C., Torp, T., Edwards, S.G., Dill-Macky, R., Hofgaard, I.S., 2018. HT-2 and T-2 toxins in Norwegian oat grains related to weather conditions at different growth stages. Eur. J. Plant Pathol. 151, 501–514.

Horvatovich, K., Hafner, D., Bodnar, Z., Berta, G., Hancz, C., Dutton, M., Kovacs, M., 2013. Dose-related genotoxic effect of T-2 toxin measured by comet assay using peripheral blood mononuclear cells of healthy pigs. Acta Vet. Hung. 61, 175–186.

Kaut, O., Ramirez, A., Pieper, H., Schmitt, I., Jessen, F., Wüllner, U., 2014. DNA methylation of the TNF-α promoter region in peripheral blood monocytes and the cortex of human Alzheimer's disease patients. Dement Geriatr. Cogn. 38, 10–15.

Lawson, B., Robinson, R.A., Toms, M.P., Risely, K., MacDonald, S., Cunningham, A.A., 2018. Health hazards to wild birds and risk factors associated with anthropogenic food provisioning. Philos. T. R. Soc. B. 373.

Li, S.J., Pasmans, F., Croubels, S., Verbrugghe, E., Van Waeyenberghe, L., Yang, Z., Haesebrouck, F., Martel, A., 2013. T-2 toxin impairs antifungal activities of chicken macrophages against Aspergillus fumigatus conidia but promotes the pro-inflammatory responses. Avian Pathol. 42, 457–463.

Li, S.Y., Cao, J.L., Shi, Z.L., Chen, J.H., Zhang, Z.T., Hughes, C.E., Caterson, B., 2008. Promotion of the articular cartilage proteoglycan degradation by T-2 toxin and selenium protective effect. J. Zhejiang Univ. - Sci. B. 9, 22–33.

Liu, X., Huang, D., Guo, P., Wu, Q., Dai, M., Cheng, G., Hao, H., Xie, S., Yuan, Z., Wang, X., 2017a. PKA/CREB and NF-kappaB pathway regulates AKNA transcription: a novel insight into T-2 toxin-induced inflammation and GH deficiency in GH3 cells. Toxicology 392, 81–95.

Liu, X.L., Guo, P., Liu, A.M., Wu, Q.H., Xue, X.J., Dai, M.H., Hao, H.H., Qu, W., Xie, S.Y., Wang, X., et al., 2017b. Nitric oxide (NO)-mediated mitochondrial damage plays a critical role in T-2 toxin -induced apoptosis and growth hormone deficiency in rat anterior pituitary GH3 cells. Food Chem. Toxicol. 102, 11–23.

Lu, A.R., Wang, J.M., Sun, W.H., Huang, W.R., Cai, Z.M., Zhao, G.P., Wang, J., 2019. Reprogrammable CRISPR/dCas9-based recruitment of DNMT1 for site-specific DNA demethylation and gene regulation. Cell Discov. 5, 22.

Luo, J.C., Li, X.W., Li, X.R., He, Y.M., Zhang, M.D., Cao, C.Y., Wang, K., 2018. Selenium-Rich Yeast protects against aluminum-induced peroxidation of lipide and inflammation in mice liver. Biometals 31, 1051–1059.

Matejova, I., Faldyna, M., Modra, H., Blahova, J., Palikova, M., Markova, Z., Franc, A., Vicenova, M., Vojtek, L., Bartonkova, J., et al., 2017. Effect of T-2 toxin-contaminated diet on common carp (Cyprinus carpio L.). Fish Shellfish Immunol. 60, 458–465.

Matt, S.M., Lawson, M.A., Johnson, R.W., 2016. Aging and peripheral lipopolysaccharide can modulate epigenetic regulators and decrease IL-1beta promoter DNA methylation in microglia. Neurobiol. Aging 47, 1–9.

Meszaros, A., Weidinger, A., Dumitrescu, S., Mullebner, A.V., Duvigneau, J.C., Kozlov, A.V., 2017. The impact of pro-inflammatory cytokines on ROS mediated liver damage. Free Radical Biol. Med. 112 206-206.

Morcia, C., Tumino, G., Ghizzoni, R., Badeck, F.W., Lattanzio, V.M.T., Pascale, M., Terzi, V., 2016. Occurrence of Fusarium langsethiae and T-2 and HT-2 toxins in Italian malting barley. Toxins 8.

Nakamura, K., Aizawa, K., Aung, K.H., Yamauchi, J., Tanoue, A., 2017. Zebularine upregulates expression of CYP genes through inhibition of DNMT1 and PKR in HepG2 cells. Sci. Rep.Uk. 7.

Nicolia, V., Cavallaro, R.A., Lópezgonzález, I., Maccarrone, M., Scarpa, S., Ferrer, I., Fuso, A., 2017. DNA methylation profiles of selected pro-inflammatory cytokines in alzheimer disease. J. Neuropathol. Exp. Neurol. 76, 27–31.

Notley, C.A., Jordan, C.K., McGovern, J.L., Brown, M.A., Ehrenstein, M.R., 2017. DNA methylation governs the dynamic regulation of inflammation by apoptotic cells during efferocytosis. Sci. Rep. Uk. 7.

NRC (National Research Council), 2004. The development of science based guidelines for laboratory animal care. In: Proceedings of the November 2003 International Workshop. National Academy Press, Washington, DC.

Pacis, A., Mailhot-Leonard, F., Tailleux, L., Randolph, H.E., Yotova, V., Dumaine, A., Grenier, J.C., Barreiro, L.B., 2019. Gene activation precedes DNA demethylation in response to infection in human dendritic cells. P. Natl. Acad. Sci. USA. 116, 6938–6943.

Page, A., Paoli, P., Salvador, E.M., White, S., French, J., Mann, J., 2016. Hepatic stellate cell transdifferentiation involves genome-wide remodeling of the DNA methylation landscape. J. Hepatol. 64, 661–673.

Paterson, R.R.M., Venancio, A., Lima, N., Guilloux-Benatier, M., Rousseaux, S., 2018. Predominant mycotoxins, mycotoxigenic fungi and climate change related to wine. Food Res. Int. 103, 478–491.

Ravindran, J., Agrawal, M., Gupta, N., Rao, P.V.L., 2011. Alteration of blood brain barrier permeability by T-2 toxin: role of MMP-9 and inflammatory cytokines. Toxicology 280, 44–52.

Sehata, S., Kiyosawa, N., Atsumi, F., Ito, K., Yamoto, T., Teranishi, M., Uetsuka, K., Nakayama, H., Doi, K., 2005. Microarray analysis of T-2 toxin-induced liver, placenta and fetal liver lesions in pregnant rats. Exp. Toxicol. Pathol. 57, 15–28.

Shakya, R., Gonda, T., Quante, M., Salas, M., Kim, S., Brooks, J., Hirsch, S., Davies, J., Cullo, A., Olive, K., et al., 2013. Hypomethylating therapy in an aggressive stroma-rich model of pancreatic carcinoma. Cancer Res. 73, 885–896.

Shen, J., Wu, S.G., Guo, W., Liang, S.S., Li, X.Y., Yang, X.J., 2017. Epigenetic regulation of pro-inflammatory cytokine genes in lipopolysaccharide -stimulated peripheral blood mononuclear cells from broilers. Immunobiology 222, 308–315.

Shinozuka, J., Miwa, S., Fujimura, H., Toriumi, W., Doi, K., 2009. T-2 toxin-induced hepatotoxicity in mice: histopathology and gene expression profile. Toxicol. Pathol. 37, 134–135.

Slobodchikova, I., Vuckovic, D., 2018. Liquid chromatography - high resolution mass spectrometry method for monitoring of 17 mycotoxins in human plasma for exposure studies. J. Chromatogr., A 1548, 51–63.

Smith, M.C., Hymery, N., Troadec, S., Pawtowski, A., Coton, E., Madec, S., 2017. Hepatotoxicity of fusariotoxins, alone and in combination, towards the HepaRG human hepatocyte cell line. Food Chem. Toxicol. 109, 439–451.

Suneja, S.K., Wagle, D.S., Ram, G.C., 1987. Liver lipid metabolism in T-2 toxicosis. I. Effects of a single dose feeding of T-2 toxin to rats. Arch. Toxicol. 60, 382–387.
Tamimi, S.O., Natour, R.M., Halabi, K.S., 1997. Individual and combined effects of chronic T-2 toxin and aflatoxin B1 mycotoxins on rat lives and kidney. Arab Gulf J. Sci. Res. 15, 717–732.
Tanaka, T., Abe, H., Kimura, M., Onda, N., Mizukami, S., Yoshida, T., Shibutani, M., 2016. Developmental exposure to T-2 toxin reversibly affects postnatal hippocampal neurogenesis and reduces neural stem cells and progenitor cells in mice. Arch. Toxicol. 90, 2009–2024.
Tsuchida, M., Miura, T., Shimizu, T., Aibara, K., 1984. Elevation of thiobarbituric acid values in the rat-liver intoxicated by T-2-toxin. Biochem. Med. 31, 147–166.
Wang, J., Yan, X.X., Nesengani, L.T., Ding, H., Yang, L.Y., Lu, W.F., 2018a. LPS-induces IL-6 and IL-8 gene expression in bovine endometrial cells "through DNA methylation. Gene 677, 266–272.
Wang, Y.J., Nie, J.Y., Yan, Z., Li, Z.X., Cheng, Y., Farooq, S., 2018b. Multi-mycotoxin exposure and risk assessments for Chinese consumption of nuts and dried fruits. J. Integr. Agr. 17, 1676–1690.
Wu, W., Zhou, H.R., Bursian, S.J., Link, J.E., Pestka, J.J., 2016. Emetic responses to T-2 toxin, HT-2 toxin and emetine correspond to plasma elevations of peptide YY3-36 and 5-hydroxytryptamine. Arch. Toxicol. 90, 997–1007.
Wu, X.J., Zhang, Y., 2017. TET-mediated active DNA demethylation: mechanism, function and beyond. Nat. Rev. Genet. 18, 517–534.
Yang, F., Zhou, S., Wang, C.D., Huang, Y., Li, H.W., Wang, Y., Zhu, Z.N., Tang, J., Yan, M.N., 2017. Epigenetic modifications of interleukin-6 in synovial fibroblasts from osteoarthritis patients. Sci. Rep. Uk. 7.
Yang, J., Ikezoe, T., Nishioka, C., Nobumoto, A., Yokoyama, A., 2013. IL-1beta inhibits self-renewal capacity of dormant CD34(+)/CD38(-) acute myelogenous leukemia cells in vitro and in vivo. Int. J. Cancer 133, 1967–1981.
Yu, J., Hua, R., Zhang, Y., Tao, R., Wang, Q., Ni, Q., 2019. DNA hypomethylation promotes invasion and metastasis of gastric cancer cells by regulating the binding of SP1 to the CDCA3 promoter. J. Cell. Biochem. https://doi.org/10.1002/jcb.28993.
Yuan, K., Lei, Y., Chen, H.N., Chen, Y., Zhang, T., Li, K., Xie, N., Wang, K., Feng, X., Pu, Q., et al., 2016. HBV-induced ROS accumulation promotes hepatocarcinogenesis through Snail-mediated epigenetic silencing of SOCS3. Cell Death Differ. 23, 616–627.
Zhang, J., Wang, C., Ha, X., Li, W., Xu, P., Gu, Y., Wang, T., Wang, Y., Xie, J., 2016. The DNA methylation of TNF-aplha, MCP-1, and adiponectin in visceral adipose tissue is related to type 2 diabetes in Xinjiang Uygur population. J. Diabetes 9, 699.
Zhang, J., Zhang, H., Liu, S.L., Wu, W.D., Zhang, H.B., 2018a. Comparison of anorectic potencies of type A trichothecenes T-2 toxin, HT-2 toxin, diacetoxyscirpenol, and neosolaniol. Toxins 10.
Zhang, X.Y., Wang, Y., Velkov, T., Tang, S.S., Dai, C.S., 2018b. T-2 toxin-induced toxicity in neuroblastoma-2a cells involves the generation of reactive oxygen, mitochondrial dysfunction and inhibition of Nrf2/HO-1 pathway. Food Chem. Toxicol. 114, 88–97.
Zhou, X.R., Wang, Z.L., Chen, J.H., Wang, W., Song, D.Q., Li, S.Y., Yang, H.J., Xue, S.H., Chen, C., 2014. Increased levels of IL-6, IL-1 beta, and TNF-alpha in Kashin-Beck disease and rats induced by T-2 toxin and selenium deficiency. Rheumatol. Int. 34, 995–1004.